BABEȘ – BOLYAI UNIVERSITY
Faculty of Chemistry and Chemical Engineering

PhD Thesis Summary

Integrating process intensification with advanced control strategies for improved carbon capture plant performance

PhD Candidate: Eng. Flavia-Maria Ilea
Supervisor: Prof. PhD. Eng. Călin-Cristian Cormoș

Cluj-Napoca
2025

Summary table of contents

Keywords: carbon dioxide capture, fluidised bed absorption, mathematical modelling, plant control strategies, process intensification, techno-economic analysis

Thesis table of contents

1. Introduction

1.1 Motivation and background

The most common greenhouse gases produced due to human activities are carbon dioxide (CO_2), methane (CH_4), nitrous oxide (N_2O), and fluorinated gases, including hydrofluorocarbons, perfluorocarbons, sulphur hexafluoride, and nitrogen trifluoride [1]. Of the previously mentioned, CO_2 is the most abundant, both in Romania [2] and worldwide [3], as shown in Figure 1.

Figure 1. *Romania and global greenhouse gas emissions by gas*

As shown in Table 1, carbon dioxide has a prolonged atmospheric lifetime, with its persistence reaching up to 200 years [4]. This extended residence time emphasises the long-term impact of CO_2 on the Earth's climate system. As the gas remains in the atmosphere for centuries, it contributes to the enhanced greenhouse effect. This ultimately leads to the global warming phenomenon [5].

Table 1. *GWP for the main anthropogenic GHG [6]*

GHG	Atmospheric lifetime [years]	Global Warming Potential	Primary Sources
Carbon Dioxide (CO_2)	50 – 200	1	Fossil fuels, land use change, cement industry
Methane (CH_4)	12 ± 3	21	Fossil fuels, agriculture
Nitrous oxide (N_2O)	120	310	Agriculture

Hydrofluorocarbons (HFCs)	1.5 – 209	150 – 11700	Alternative to ozone, substance depletion
Perfluorocarbons (PFCs)	2600 – 50000	6500 – 9200	Aluminium production, semiconductor manufacture
Sulphur Hexafluoride (SF_6)	3200	23900	Electric power transmission, magnesium, and semiconductor industry

Apart from the persistence of CO_2, its diverse and widely-spread anthropogenic sources need to be taken into account [7]. These sources can be categorised into four main sectors: heat and power, industry, transport, and residential [8]. This is shown in Figure 2.

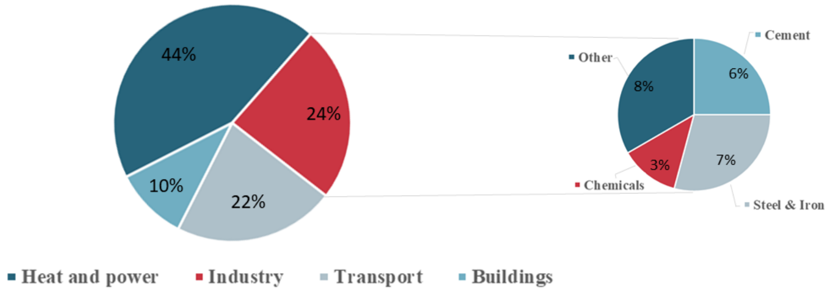

Figure 2. *Anthropogenic sources of carbon dioxide (2024)*

The ongoing expansion of the industrial sector, coupled with rising global energy demand, has led to a steady and significant increase in carbon dioxide emissions over the course of the last years [9]. This increase in emissions can be seen in Figure 3 [10].

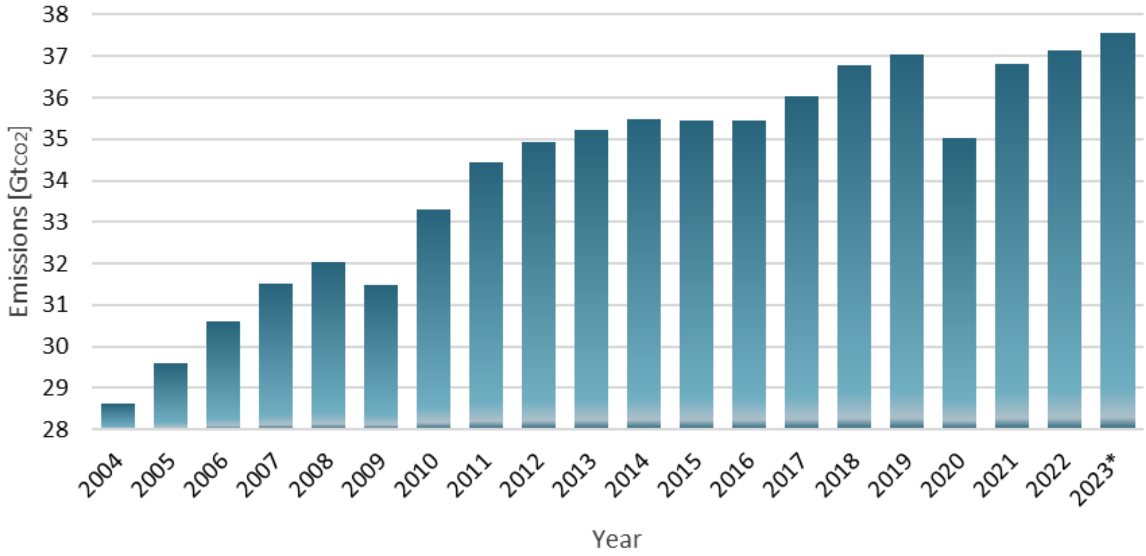

Figure 3. *Evolution of CO_2 emissions*

In Figure 3, the values axis has been adjusted to begin at 28 in order to enhance the visibility of variations from year to year within the observed timeframe. This allows for a clearer view of the recent data. As shown, there has been a 30% increase in carbon dioxide emissions over the last 20 years. The data also show the impact of the first year of the COVID-19 pandemic (2020), when, due to confinement measures and widespread limitations on economic activity, there was a significant decrease in carbon dioxide emissions compared to the years before and after [11].

Despite this, the recent record-high level of CO_2 emissions shows the persistent challenges faced by the global community in transitioning towards sustainable development [12]. This trend highlights the importance of making efforts to adopt cleaner energy sources and enhance energy efficiency in order to stop the ongoing increase in greenhouse gas emissions [13].

The achievement of net-zero emissions by 2050 is connected to the goal of meeting either of the 1.5°C and 2°C targets [14]. Considering the ongoing initiatives, there are several different policy scenarios, as shown in Figure 4 [15].

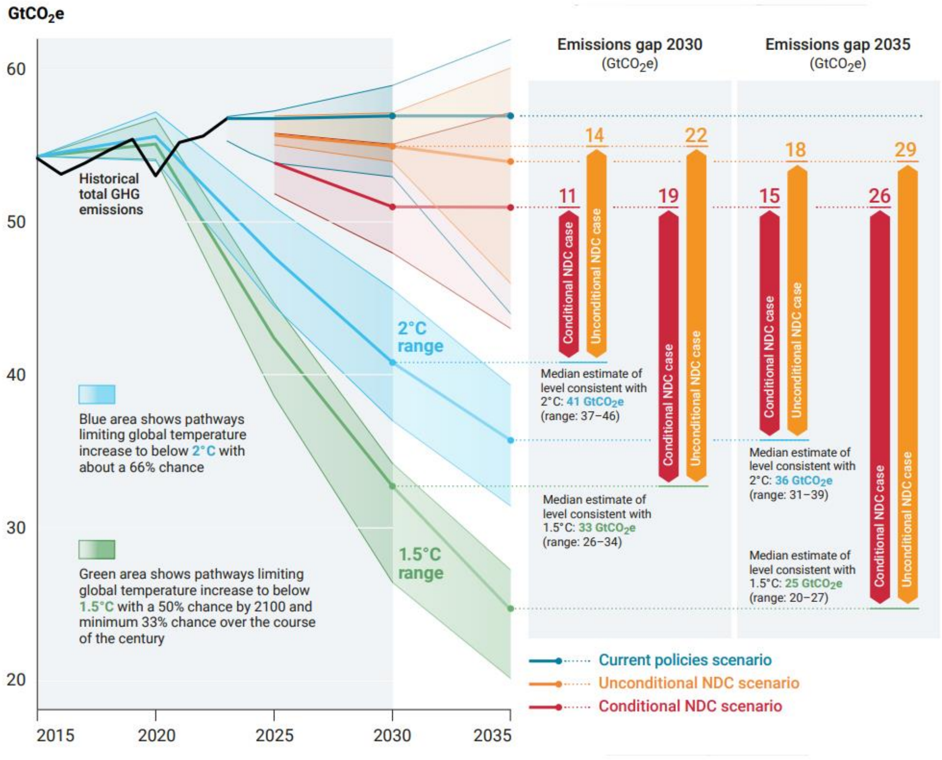

Figure 4. *Global GHG emissions under different scenarios*

Figure 4 highlights the trajectory of global greenhouse gas emissions under different policy scenarios and the emissions gap that must be closed to meet international climate goals. The historical emissions trend, shown by the black line, indicates a steady increase, while future projections diverge depending on the level of climate action taken. The figure illustrates three scenarios: current policies, unconditional Nationally Determined Contributions (NDCs), and conditional NDCs, each representing different levels of commitments and implementation [16].

These figures indicate that even if all conditional NDCs are fully implemented, emissions reductions still fall short of what is necessary, reinforcing the need for more ambitious climate policies and accelerated global action. [17].

Taking all the aforementioned information into consideration, transitioning from fossil fuel-based energy production to energy generation using non-fossil and renewable sources would help achieve the goal of net-zero CO_2 emissions [18]. This shift is needed for combating climate change and reduce the environmental impact of energy production. However, the current demand for electricity driven by ongoing economic growth cannot be met only through renewable energy sources [19]. This is mainly due to their inherent variability and intermittency (i.e., fluctuations based on weather conditions and time of the day) [20]

One solution that allows for the continued use of fossil fuels while mitigating CO_2 emissions is carbon capture and storage (CCS) [21]. CCS involves the capture of CO_2 from emission sources, such as power plants and industrial processes [22]. The captured CO_2 is then transported to a designated storage site, where it can be injected into geological formations (i.e. depleted oil and gas reservoirs or deep saline aquifers) for permanent storage [23].

These technologies are designed to capture CO_2 before it is released into the atmosphere, enabling its storage or utilisation in various industrial applications [21]. The primary carbon capture methods include post-combustion capture, pre-combustion capture, and oxyfuel combustion, each with distinct processes and applications (Figure 5) [24].

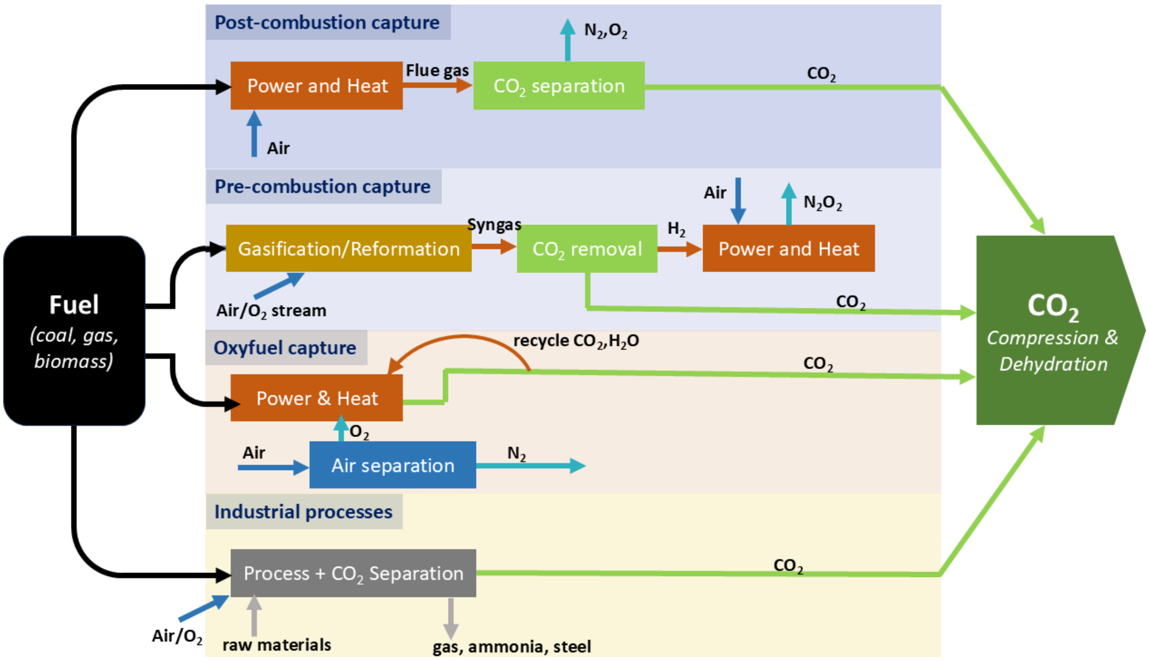

Figure 5. *Carbon dioxide capture technologies overview*

In addition to these primary methods, several emerging carbon capture technologies aim to improve efficiency and reduce costs [25]. Chemical looping combustion (CLC) is a novel approach that uses metal oxides to transfer oxygen for combustion, while separating CO_2 in the process [26]. Direct air capture (DAC) technologies are also gaining attention, as they can remove CO_2 directly from the atmosphere, offering a potential solution for addressing legacy emissions [27]. Apart from the previously mentioned capture methods, advancements in solvent and membrane technologies are enhancing the efficiency and viability of carbon capture systems [28].

1.2 Gas-liquid carbon dioxide absorption

Gas-liquid absorption is a vastly used approach for post-combustion carbon capture, relying on the interaction between CO_2 and liquid solvents to facilitate separation. The most used solvents are amine-based aqueous solutions. However, they also present challenges, including solvent degradation, corrosion, and high energy demands for regeneration [29]. Beyond amines, other solvent systems have been explored to improve efficiency and reduce operational costs. An overview of existing solvent options is presented in Table 2 [30].

Table 2. *Overview of existing solvent options for carbon capture*

Solvent type	Examples	Advantages	Disadvantages
Primary Amines	MEA Monoethanolamine	· High reactivity with CO_2 · Technologically mature · Solvent availability	· High regeneration energy · Solvent degradation · Corrosion issues
Secondary Amines	DEA Diethanolamine	· Lower regeneration energy · Less corrosive	· Slower absorption kinetics
Tertiary Amines	MDEA Methyl diethanolamine	· Low regeneration energy · Less corrosive	· Slow reaction with CO_2 · Requires activator for fast absorption

Sterically Hindered Amines	AMP 2-Amino-2-methyl-1-propanol	· High CO_2 capacity · Low energy penalty	· High solvent cost · Low absorption rate · Requires activator
Physical Solvents	Selexol™, Rectisol®	· Effective at high pressure · No chemical reaction	· Not effective at low CO_2 partial pressures · High solvent loss
Aqueous Ammonia	NH_3 solution	· Low regeneration energy · High CO_2 capture capacity	· Volatility of ammonia · Toxicity · Fouling (salt formation)
Ionic Liquids	Imidazolium-based ILs	· Negligible vapor pressure · Tuneable properties	· Expensive · High viscosity · Low CO_2 diffusivity
Phase-Change Solvents	CESAR1 Mixed amine systems	· Lower energy due to two-phase behaviour during regeneration	Complex design Requires control strategies
Blended Amines	MEA + MDEA AMP + PZ	· Optimized performance · High reactivity · Low energy penalty	· Risk of instability · Need for careful blend ratio
Alkaline solvents	Sodium hydroxide aqueous solution	· High absorption capacity · Forms stable Na_2CO_3 or $NaHCO_2$ · Widely available	· Regeneration only possible with very high energy penalty · Corrosive · Need for precipitate management

1.3 Process intensification technologies

Another approach to mitigating the disadvantages of existing carbon capture technologies is the adoption of innovative contacting methods that enhance the efficiency of the absorption process. Process intensification techniques, such as structured packings, microchannel reactors, high-gravity field reactors, and membrane contactors, can improve the mass transfer between CO_2 and the solvent, leading to more effective capture [31,32]. Integrating fluidised bed absorbers and centrifugal contactors can increase the interfacial area for gas-liquid interactions, resulting in faster absorption rates [33]. These advancements can reduce the size and cost of capture systems, lower energy consumption, and improve overall process efficiency [34].

Table 3 gives an overview on both the advantages and disadvantages and characteristics of existing process intensification technologies.

Table 3. *Overview of existing process intensification technologies*

Technology	Mass transfer rate [mol/(m²·s)]	Advantages	Disadvantages
Packed Bed	0.001 – 0.01	· Proven efficiency · Scalable · Predictable	· Bulky structure · High pressure drop · Flooding risk
Spray Column	~0.001	· Simple design · Low pressure drop	· Low efficiency · Droplet coalescence
Bubble Column	0.001 – 0.005	· Easy to operate · No internals	· Low throughput · Gas slip
Membrane Contactor	0.01 – 0.1	· Very compact · No flooding	· Wetting · Fouling · High cost
Rotating Packed Bed	0.05 – 0.5	· High intensification · Compact	· Complexity · Vibration · Scaling

TCA	0.1 – 0.5+	· Fast absorption · Very compact	· Experimental · Control complexity
Microchannel	0.1 – 1.0	· Ultra-compact · Heat/mass transfer high efficiency	· Expensive · Fouling · Difficult scale-up
Monolithic Absorber	~0.01 – 0.1	· Low pressure drop · Robust structure	· Wetting limitations · Manufacturing complexity

Turbulent contact absorbers are an innovative approach to improving the efficiency of gas-liquid absorption processes, particularly in the context of carbon capture. These absorbers are designed to create high levels of turbulence within the absorption column, which enhances the mixing of the gas and liquid phases, thereby increasing the rate of mass transfer [35]. This type of equipment, used as a three-phase gas-solid-liquid absorption column, is detailed in Chapter 3 of this thesis.

1.4 Control strategies for carbon capture processes

The post-combustion carbon capture process using amines, particularly MEA, is widely recognised as one of the leading technologies for CO_2 capture. This method employs the use of both absorption and stripping columns. In this setup, CO_2 is initially absorbed by an amine solvent in the absorber and then released as a high-concentration CO_2 stream at the top of the stripper. During this process, the solvent is regenerated in the desorption column and then returned to the absorber. The efficiency of this technology, both in terms of CO_2 removal and economic performance, depends on the operational flexibility of the carbon capture plant. Such flexibility can be achieved through careful plant design and robust control systems [36].

Table 4 presents an overview of the existing control strategies presented before and a comparison between their advantages and disadvantages.

When designing a control strategy for the carbon capture plant, each of the aforementioned factors needs to be taken into consideration. Chapter 4 of this thesis presents different control approaches and their respective performances.

Table 4. *Overview of different control strategies for carbon capture units*

Control strategy	**Advantages**	**Disadvantages**	**Common application**
Basic Feedback Control	· Simple · Well understood · Low implementation cost	· Delayed response · May struggle with disturbances	Industrial packed bed systems
Cascade Control	· Improved stability · Better disturbance rejection	· Requires accurate models and tuning	Stripper column energy control
Ratio Control	· Optimal stoichiometry · Fast-responding	· Needs accurate flow measurements · Limited flexibility	Amine circulation systems
Feedforward Control	· Pre-emptive correction · Good for known disturbances	· Requires accurate process model and sensors	CO_2-rich flue gas handling
Model Predictive Control	· Handles constraints · Multivariable · Predictive	· Complex implementation · High computational needs	Advanced pilot and demo-scale systems
Inferential Control	· Reduces need for expensive gas analysers	· Model-dependent · Sensitive to drift or sensor error	Real-time lean/rich loading management
Adaptive Control	· Adjusts to process changes · Good under varying loads	· Complex · Potential stability issues if not tuned properly	Variable flue gas conditions (e.g., cement)
Decentralized Control	· Easier to design per-unit · No central coordination needed	· Can result in interaction issues · Less efficient	Smaller units or legacy systems
Real-Time Optimization	· Holistic optimization	· Computationally intensive · Long response time	Smart plant-wide operation

2. Assessment methodology

2.1 Mathematical modelling and simulation

The modelling and simulation of carbon capture processes have an important role in evaluating the efficiency, feasibility, and scalability of different technologies. As global efforts to mitigate climate change intensify, accurate process models provide valuable insights into the optimisation of carbon capture systems, helping industries and policymakers make informed decisions. The software tools used in this work for the development, implementation and simulation of complex mathematical models and process flow modelling were MATLAB/Simulink and ChemCAD.

MATLAB (Matrix Laboratory) is a high-level programming environment widely used for numerical computing, data analysis, and simulation. Developed by MathWorks, MATLAB provides numerous tools for solving complex mathematical problems, making it a useful choice for engineers, scientists, and researchers. Simulink, a powerful toolbox within MATLAB, provides a variety of ODE (Ordinary Differential Equation) solvers for simulating dynamic systems. These solvers are essential for solving time-dependent differential equations [37].

MATLAB and its Simulink extension was used in this work for the dynamic simulation of packed bed absorption columns, gas-solid-liquid fluidised bed columns, an absorption/stripping carbon capture unit and different control strategies.

CHEMCAD is a process simulation software widely used in chemical engineering for designing, analysing, and optimising chemical processes. Developed by Chemstations, it provides a comprehensive environment for steady-state and dynamic simulations, making it a useful tool for industries such as petrochemicals, pharmaceuticals, and environmental engineering.

CHEMCAD offers a range of functionalities that enhance process simulation and analysis:

- Process Flow Simulation – Allows users to design and simulate complete chemical process flowsheets.
- Thermodynamic Modelling – Supports various thermodynamic packages for accurate property calculations.
- Equipment Sizing & Rating – Helps engineers size process equipment such as absorbers, heat exchangers, and distillation columns.
- Heat & Mass Balance Calculations – Ensures accurate energy and material balance computations.

- Dynamic Simulation – Enables time-dependent analysis of process behaviour, which is useful for transient studies in carbon capture systems [192].

The software also provides built-in economic analysis tools that help engineers evaluate the financial feasibility of a project by estimating capital costs, operating costs, and energy consumption. This capability is particularly useful for assessing the economic viability of carbon capture technologies, where costs related to equipment, utilities, and chemicals are major considerations [38].

Equipment Cost Estimation is based on databases that incorporate cost correlations for common process equipment such as absorbers, heat exchangers, compressors, and distillation columns. Users can also input equipment specifications (i.e. construction material, pressure rating, capacity) to get an estimate of capital expenditure (CAPEX).

CHEMCAD was used in this thesis to perform the total mass balance and component mass balance within a carbon capture unit. Additionally, it was employed for flow simulation and cost estimation of each individual equipment unit involved in the process.

2.2 Regression analysis

Regression analysis is a statistical method used to examine the relationship between one or more independent variables and a dependent variable. It helps in understanding how changes in independent variables influence the dependent variable, making it a tool in mathematical modelling and data analysis. This technique is widely used across various fields, such as economics, finance, medicine, and machine learning, to analyse trends, make forecasts, and identify key factors affecting an outcome [39].

In this work, regression analysis was used in order to develop equations and determine the appropriate coefficients for carbon capture process parameters such as: effective mass transfer area, pressure drop and fluidised bed expansion, detailed in Chapter 3.

2.3 Box-Behnken Design of Experiment

The Box-Behnken Design (BBD) is a response surface methodology (RSM) used in experimental design to optimise processes with multiple independent variables. It was developed by George E. P. Box and Donald Behnken in 1960 as an efficient way to explore quadratic response surfaces while reducing the number of experimental runs compared to full factorial designs. BBD is particularly useful in fields such as engineering, chemistry, and pharmaceuticals, where process optimisation is very important [40].

For three considered variables, the Box Benken DoE proposes the use of 3 values for each: a lower value (represented by -1), a middle value (represented as 0) and a higher value (represented as 1). The way the experiments are chosen is presented in Table 5 [41]. This is the case that was used in Chapter 4 of this thesis.

Table 5. *Considered cases for a 3-variable DoE*

Case	Variable 1	Variable 2	Variable 3
1	-1	-1	0
2	1	-1	0
3	-1	1	0
4	1	1	0
5	-1	0	-1
6	1	0	-1
7	-1	0	1
8	1	0	1
9	0	-1	-1
10	0	1	-1
11	0	-1	1
12	0	1	1
13	0	0	0

2.4 Performance indices

In order to assess and compare the performance of different carbon capture systems, several performance indices were considered. These indices help quantify not only the carbon capture yield of each system but also its viability and energy efficiency.

In this study, the carbon capture rate is calculated as the quantity of CO_2 that leaves the desorber per the quantity of CO_2 that enters the CC plant:

$$CC = \frac{CO_2(captured)}{CO_2(absorber\ inlet)} \cdot 100 \tag{E1}$$

Calculated like this, the carbon capture rate offers an insight regarding the overall process performance. This is due to the fact that this measure is not only connected to the absorption unit but also to the desorber.

The absorption rate is defined as the ratio between the quantity of absorbed CO_2 per quantity of CO_2 that enters in the CC plant:

$$R_{abs} = \frac{CO_2(absorber\ inlet) - CO_2(absorber\ outlet\ gas)}{CO_2(absorber\ inlet)} \cdot 100 \quad \text{(E2)}$$

The energy performance index is defined as the quantity of energy (in MJ) needed to capture one kilogram of carbon dioxide:

$$E_P = \frac{Q_r}{CO_2(captured)} \quad \text{(E3)}$$

The key performance indices used for the assessment and evaluation of the control strategies detailed in Chapter 4 help quantify both the efficiency of the proposed strategies and the energy performance of the system. Apart from the already mentioned indices, the following are also employed:

- Lean solvent CO_2 loading, expressed as moles of CO_2 per mole of solvent after regeneration step [mol/mol];
- Solvent circulation rate, expressed as solvent flow per unit gas flow [l/s];
- Reboiler duty stability, expressed as deviation in the reboiler heat duty [%];
- Setpoint tracking error as a measure of how closely the process follows control setpoints [error %];
- Disturbance rejection, as the time needed to return to steady state after disturbance [s];
- Controller robustness, as the sensitivity to process model mismatch or noise.

For the economical analysis several different performance indices were considered. An overview is presented in Table 6 [42].

Table 6. *Economic indices overview*

Index	Description	Unit
Levelized Cost of CO_2 Capture (LCOC)	Total cost per ton of CO_2 captured over plant lifetime	€/ton CO_2
Capital Expenditure (CAPEX)	One-time investment in equipment, installation, and infrastructure	€
Operating Expenditure (OPEX)	Annual costs: utilities (steam, electricity), labour, solvent makeup, maintenance	€/year or \$/ton CO_2

Energy Penalty	% decrease in power plant efficiency due to carbon capture	% net efficiency drop
Specific Reboiler Duty	Heat required to regenerate solvent per kg of CO_2	MJ/kg CO_2
Solvent Loss/Degradation Cost	Cost due to solvent degradation, emissions, or required replacement	€/ton CO_2 or €/kg solvent/year
Payback Period	Time to recover capital investment from savings or carbon credits	Years
Net Present Value (NPV)	Present value of future cash flows minus investment costs	€ (positive = profitable)
Internal Rate of Return (IRR)	Annualized effective return on investment	%
Plant Availability / Uptime	Operational availability of the capture system	% uptime per year
Cost of Avoided CO_2	Accounts for baseline emissions and energy penalty (better than just $/ton captured)	€/ton CO_2 avoided
Levelized Cost of Electricity (LCOE)	average cost per unit of electricity generated over the lifetime of a power plant, including all capital, operational, and fuel costs	€/MWh

Together, these indices form the backbone of any techno-economic analysis guiding deployment decisions.

Environmental performance metrics are essential to assess the sustainability of carbon capture technologies beyond their technical and economic viability. Indices such as global warming potential (GWP), water footprint, and solvent-related emissions help quantify the broader ecological impact of these systems. The global warming potential represents the total greenhouse gas emissions as CO_2 equivalent [43].

3. Gas-solid-liquid fluidised bed absorption

3.1 Process overview and experimental design

This chapter is structured around three-phase, gas-solid-liquid fluidised bed absorption for CO_2 capture, focusing on: i) the experimental evaluation of this type of process, ii) mathematical modelling and simulation, and iii) techno-economic assessment. By correlating experimental data with the developed mathematical models, the purpose of this work is to provide an analysis of the efficiency and feasibility of turbulent contact absorbers in carbon dioxide capture systems.

Turbulent contact absorbers, or three-phase fluidised bed columns, introduce a third phase, low-density inert solid particles, into the gas-liquid system. In this setup, the gas phase is the continuous phase, while the liquid phase is dispersed. The solid particles are fluidised by the upward gas flow. The main advantage of TCAs lies in their ability to intensify mass transfer by significantly increasing the effective mass transfer area [44]. The physical model of such a system is presented in Figure 6.

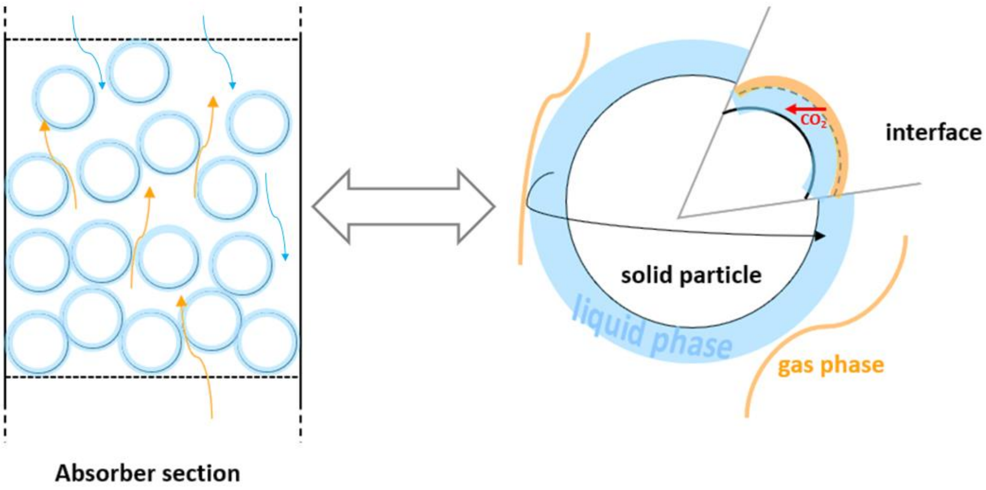

Figure 6. *Physical model of three phase fluidised bed absorption*

In the experimental setup, the gas phase was introduced at the bottom of the column, being transported by a blower. The liquid phase enters the column from the top and acts as the dispersed phase. Hence, the two phases circulate the column in counter-current. The absorber was filled with spherical hollow particles. Once the liquid enters the column, it covers each of the solid particles in a thin liquid film in which the mass transfer would take place. The experimental setup can be seen in Figure 7 [44].

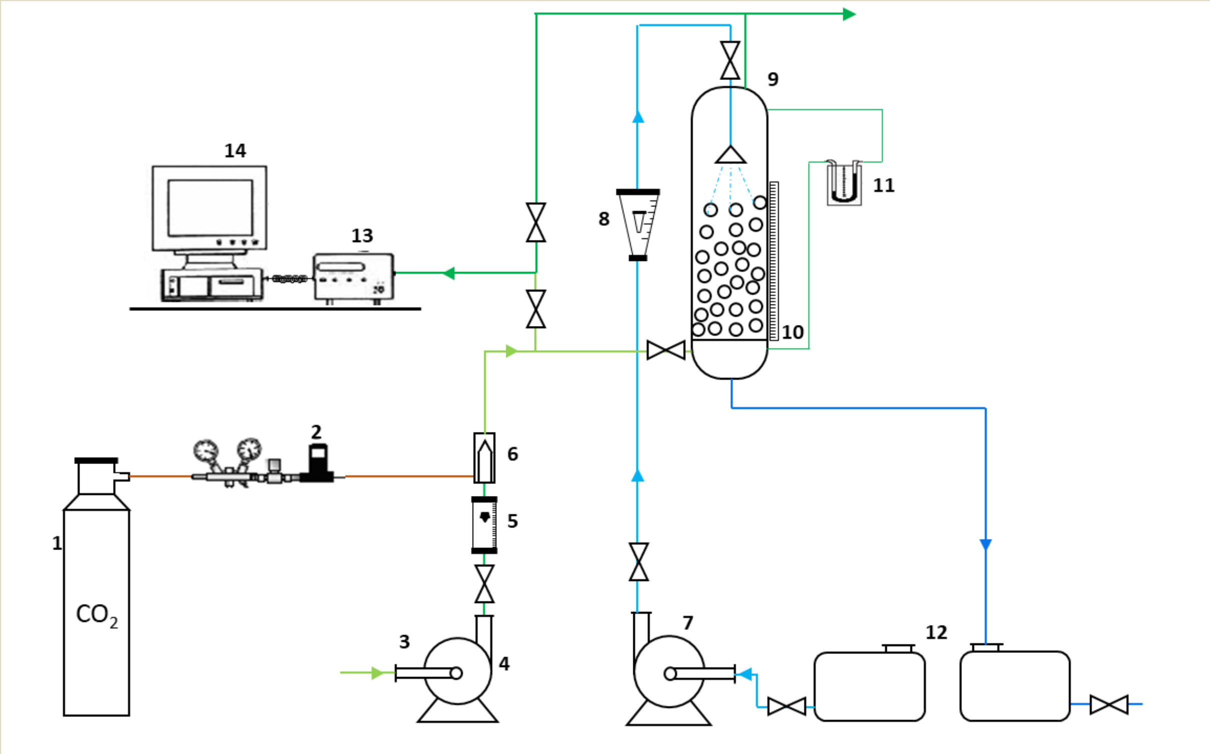

Figure 7. *Experimental setup for fluidised bed absorption*
1-carbon dioxide cylinder, 2-carbon dioxide mass flow meter, 3-air temperature controller, 4-air blower, 5-air rotameter, 6-gas mixing tube, 7-liquid pump, 8-liquid rotameter, 9-three phase fluidised bed absorber column, 10-graduatet scale, 11-manometer, 12-solution tanks, 13-gas analyser, 14-IBM computer.

3.2 Mathematical model

Developing a comprehensive mathematical model is needed for better understanding and improving the performance of three-phase fluidised bed absorption used for CO_2 capture. The proposed model focuses on both physical and chemical phenomena, including hydrodynamics, mass transfer, and chemical reaction kinetics.

In the conducted studies regarding the use of three-phase fluidization for carbon capture, three different solvents were considered: NaOH aqueous solution, NaOH and glycerol aqueous solution, and MEA aqueous solution. For each case, the kinetics of the chemical reactions between the chemical species were taken into consideration and included in the model.

The hydrodynamics model was developed taking into account existing correlations presented in the literature. It includes equations for the liquid hold-up, the fluidised bed expansion and pressure drop. These equations were developed by aligning the ones presented in literature with the experimental results through coefficient adjustments.

$$\Delta P = \rho_l \cdot g \cdot H_0 \cdot \left(\frac{H_s}{H_0}\right)^{-1.6162} \cdot Re_g^{1.4694} \cdot Ga_l^{-0.5775} \cdot Re_l^{0.6338} \cdot We_l^{0.3598} \quad \text{(E4)}$$

$$\frac{H_{sf}}{H_0} = \left(\frac{D_c}{d_p}\right)^{1.1192} \cdot \left(\frac{\rho_s}{\rho_g}\right)^{-0.3938} \cdot \left(\frac{w_g}{w_{lmf}}\right)^{0.4462} \cdot \left(\frac{w_l}{w_{lmf}}\right)^{0.1714} \quad \text{(E5)}$$

In the case of packed bed absorption columns, Billet and Schultes [45] developed correlations for estimating the partial mass transfer coefficients and the effective mass transfer area. These correlations can be easily applied to various types of packing, including both structured and random packings, by incorporating specific adjustment coefficients.

However, these correlations are not directly applicable to gas-solid-liquid fluidised bed absorption columns. The presence and movement of solid particles introduce additional turbulence, significantly influencing mass transfer behaviour. To address these challenges, a new correlation was developed for calculating the effective mass transfer area. This correlation is based on experimental results and incorporates elements from the equations proposed by Billet and Schultes as well as Rocha et al. [45,46].

$$k_l = C_l \cdot \left(\frac{g}{\vartheta_l}\right)^{\frac{1}{6}} \cdot \left(\frac{D^l_{CO_2}}{S}\right)^{0.5} \cdot w_{l_e}^{0.5} \quad \text{(E6)}$$

$$k_g = C_g \cdot \left(\frac{1}{\varepsilon - h_l}\right)^{0.5} \cdot \left(\frac{a}{S}\right)^{0.5} \cdot D^g_{CO_2} \cdot \left(\frac{w_{g_e}}{a * \mu_g}\right)^m \cdot \left(\frac{\vartheta_g}{D^g_{CO_2}}\right)^n \quad \text{(E7)}$$

$$\frac{a_e}{a} = e^{11.89} \cdot Fr_l^{-0.0152} \cdot Fr_g^{-0.2466} \cdot Ga^{-0.7174} \quad \text{(E8)}$$

In order to develop the mass and energy balance equations, the process was simplified and modelled as a lumped parameter system. This is presented in Table 7.

Table 7. *Mass and energy balance equations*

Total mass balance	$F_j^e = F_j^0 \pm w_j \cdot \frac{N_{CO_2} \cdot M_{CO_2}}{\rho_j}$
Component mass balance	$\frac{dC_i^j}{dt} = \frac{F_j^0}{w_j} \cdot C_i^{0\,j} - \frac{F_j^e}{w_j} \cdot C_i^{\,j} \pm N_i \pm N_R$
Heat balance	$\frac{dT_j}{dt} = \frac{F_j^0}{w_j} \cdot T_j^0 - \frac{F_j^e}{w_j} \cdot T_j - \frac{\Delta H_r \cdot v_r}{\rho_j \cdot cp_j} \mp \frac{h \cdot a_e \cdot (T_l - T_g)}{(\rho_j \cdot cp_j \cdot w_j)}$

The model demonstrates a strong correlation with the experimental data, as indicated by the high correlation coefficient (R>0.9).

3.3 Technical analysis

Both liquid and gas velocities also have an important impact on how the process behaves. In this system, the liquid phase, acting as the dispersed phase, is involved in determining both the hydrodynamics and the mass transfer efficiency between phases. Figure 8 illustrates the impact of liquid spray density on hydrodynamic parameters, including fluidised bed height, pressure drop, bed expansion, and the holdup of both liquid and solid phases.

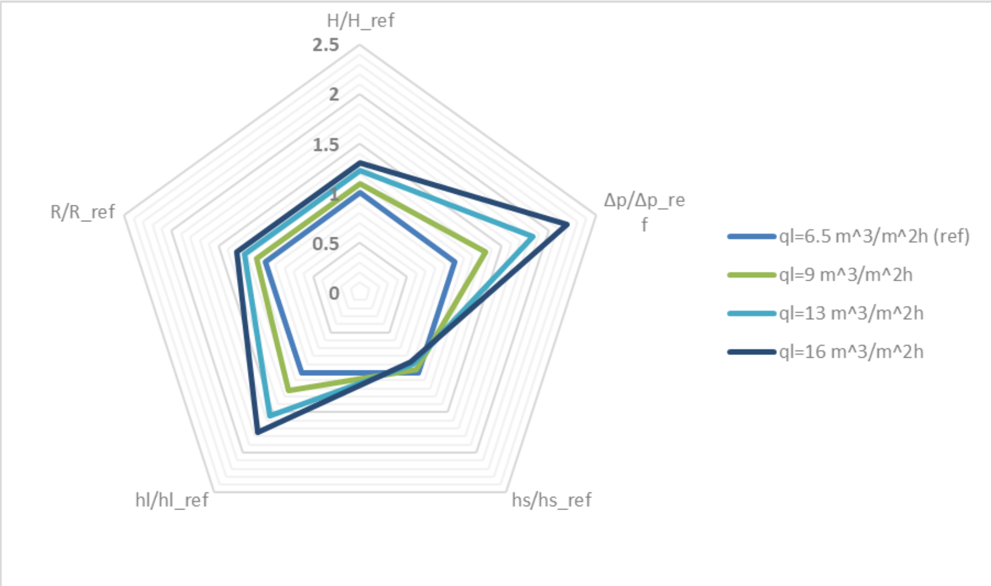

Figure 8. *Influence of liquid spray density on hydrodynamic parameters*

Higher liquid spray density results in an increase in pressure drop, indicating greater resistance to gas flow within the column. Additionally, the expansion of the fluidised bed becomes more noticeable, leading to a corresponding increase in bed height. This expansion occurs due to the enhanced interaction between the liquid phase and the gas phase, which promotes greater dispersion and upward movement within the bed. At the same time, as liquid spray density increases, the solid holdup within the system decreases. This occurs because the higher presence of liquid disrupts the packing and settling behaviour of solid particles, reducing their concentration within the bed.

The same kind of analysis was performed under the scope of changing the gas velocity. This is shown in Figure 9. For the gas velocity, the hydrodynamic parameters considered are the pressure drop and fluidised bed height. The study also shows the influence on the mass transfer through the effective mass transfer area and the efficiency of the process through the carbon capture rate. The diagram highlights that as gas velocity increases, there is a corresponding rise in the fluidised bed height and the carbon capture rate, indicating enhanced gas-liquid interaction and improved contact efficiency within the column. Additionally, the pressure drop exhibits only a slight variation, suggesting that while increased gas velocity influences other hydrodynamic factors, its impact on resistance to flow remains moderate.

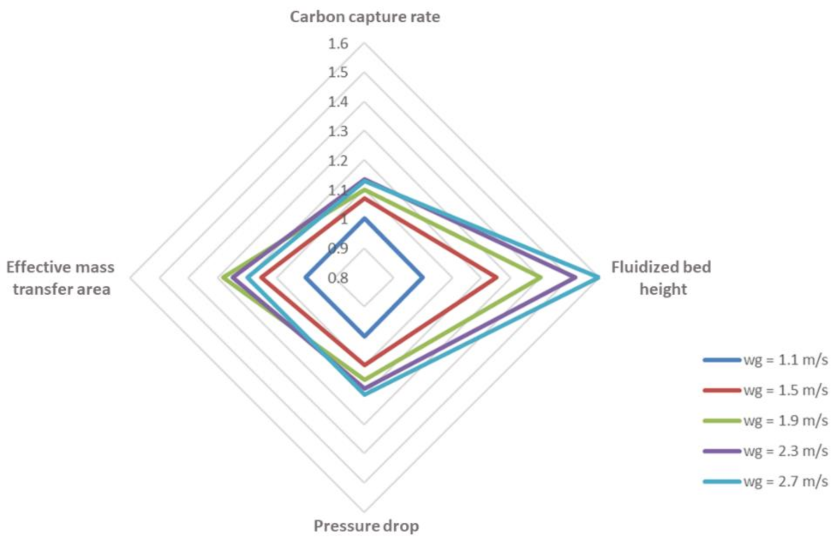

Figure 9. *Influence of gas velocity in different process parameters*

The effective mass transfer area presents a peak at an intermediate gas velocity of 1.9 m/s, after which it declines. As a result, the CO_2 capture rate reaches a plateau at higher gas velocities, indicating that increasing gas flow beyond a certain threshold does not necessarily lead to proportional improvements in absorption efficiency.

In order to be able to compare the performance of the proposed system with traditional packed bed columns, the mass transfer characteristics of each were taken into consideration. The results are presented in Table 8.

Table 8. *Mass transfer parameters for different carbon capture systems*

Model	Filling	k_l [m/s]	k_g [m/s]	a_e [m²/m³]	N_{CO2} [kmol/s]
Packed bed	**Mellapak 250Y**	$1.79 \cdot 10^{-4}$	$8.48 \cdot 10^{-2}$	123.15	$4.9 \cdot 10^{-4}$
	Rasching 50 mm	$2.36 \cdot 10^{-4}$	$4.30 \cdot 10^{-2}$	55.40	$2.5 \cdot 10^{-4}$
	Sulzer BX	$3.38 \cdot 10^{-4}$	$6.23 \cdot 10^{-2}$	224.41	$7.5 \cdot 10^{-4}$
Fluidised bed	**Spherical particles**	$1.9 \cdot 10^{-3}$	$1.59 \cdot 10^{-1}$	1985.3	$8.7 \cdot 10^{-3}$

This study revealed that the partial mass transfer coefficients for both the liquid phase (k_l) and the gas phase (k_g), as well as the effective mass transfer area (a_e), are 7 to 8 times higher in a fluidised bed reactor compared to a packed bed reactor. As a result of this intensified mass transfer behaviour, the gas-to-liquid CO_2 transfer flow shows a significant increase—up to 10 times higher in fluidised bed systems.

3.4 Scale-up and plant integration

The scale-up of absorption columns plays an important role in the transition from laboratory-scale research to industrial application. While small-scale experiments provide valuable insights into mass transfer efficiency, hydrodynamics, and operational stability, the challenge lies in ensuring that these findings can be effectively applied to larger systems without compromising performance.

The reference scenario for this study is a single-stage absorption column with a fixed bed height of 6 meters, referred to as *Case a*. To examine the effect of introducing multiple stages on column performance, a two-stage configuration is introduced: *Case b*, in which both stages have an equal static bed height (3 m each), and *Case c*, in which the static bed height decreases from the lower stage (4 m) to the upper stage (2 m). Another column configuration with three stages is divided into two cases: *Case d*, in which the fixed bed height is the same across all three stages (2 m), and *Case e*, in which the height decreases progressively from 3 m on the lower stage, to 2 m on the middle stage, and 1 m on the upper stage.

Figures 10 and 11 present the results in terms of fluidised bed height, pressure drop and carbon capture rate.

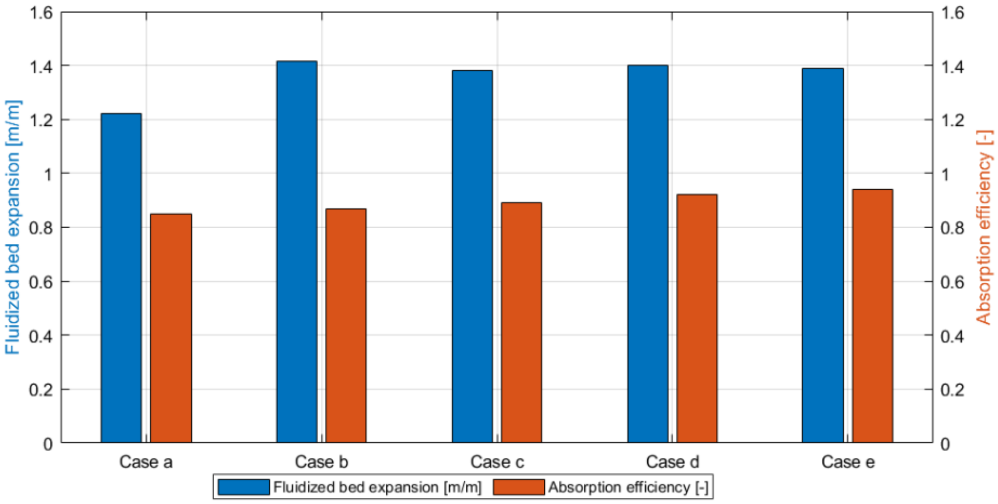

Figure 10. *Carbon capture rate and bed expansion for each considered case*

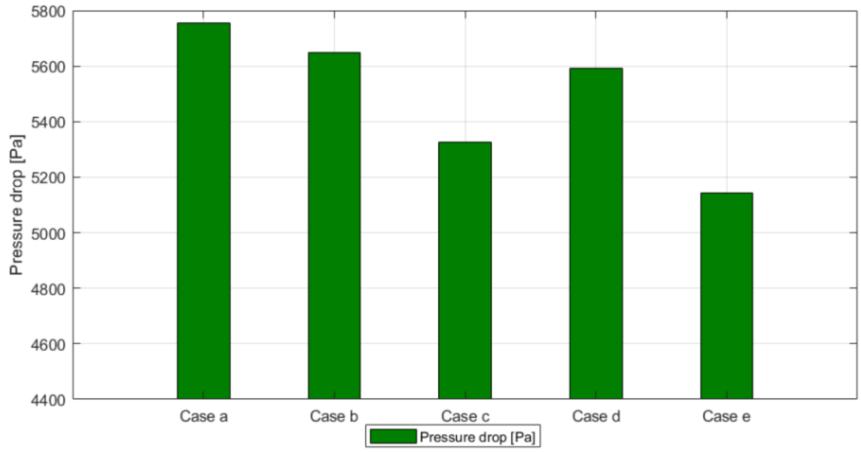

Figure 11. *Pressure drop value in each considered case*

The configuration with three stages and decreasing static bed height from the bottom to the top stage (Case e) achieves the highest carbon capture rate. Additionally, this setup exhibits lower bed expansion, suggesting that achieving high gas velocity is not a requirement for enhancing mass transfer between the liquid and gas phases. Instead, a gas velocity slightly above the minimum fluidization velocity is sufficient to generate the necessary turbulence and facilitate solid particle movement, leading to improved mass transfer efficiency.

Moreover, this configuration results in the lowest pressure drop, approximately 5150 Pa, which is significantly lower than that of other tested configurations.

An absorber with this configuration was integrated in a carbon capture unit along with a buffer tank, desorber and cross heat exchanger. This was done in order to compare the performance of this system with the regular packed bed system. The results are presented in Figure 12.

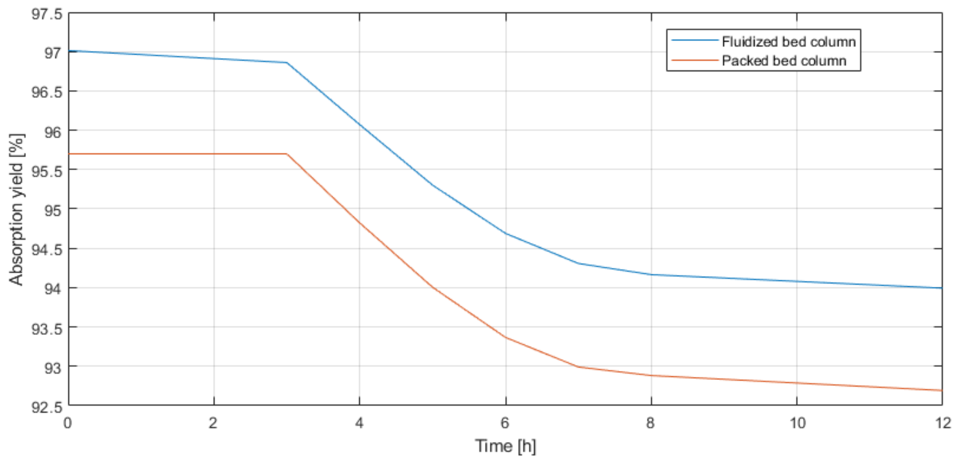

Figure 12. *Absorption efficiency under flue gas flowrate disturbance scenario*

The graph illustrates the impact of a 20% increase in influent flue gas flowrate on the absorption efficiency of a carbon capture system. Both fluidised bed and packed bed columns experience a decline in performance over time, indicating that the increased flowrate negatively affects the absorption process. However, the extent of this decline differs between the two configurations, with the fluidised bed column consistently maintaining a higher efficiency than the packed bed column. This suggests that fluidised bed technology is more resilient to fluctuations in changing flow conditions.

3.5 Economic analysis

The proposed design for the carbon capture unit of the plant is illustrated in Figure 13. The unit's flow is simulated using ChemCAD software, while the mathematical model for the absorber unit is implemented and simulated using MATLAB/Simulink.

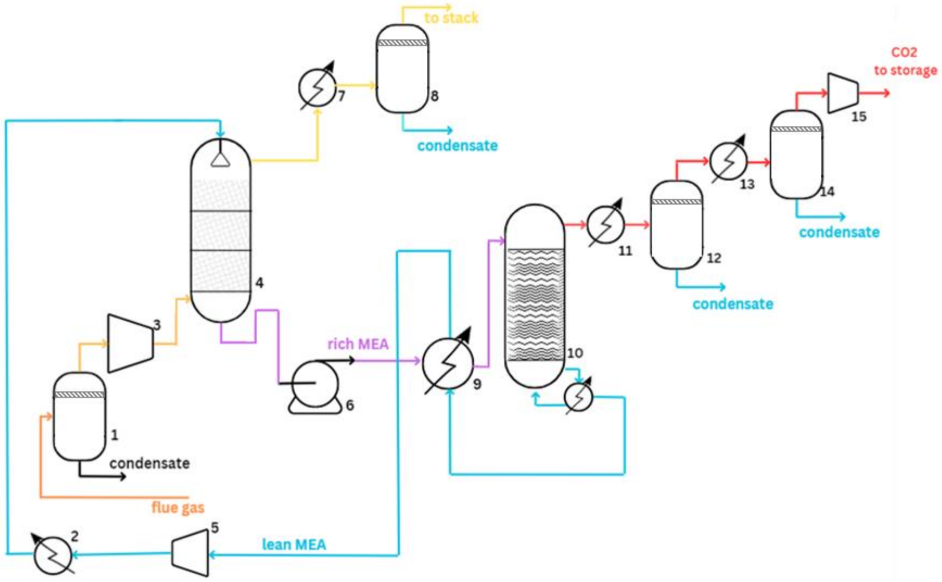

***Figure 13.** Design flowsheet of an intensified CO_2 capture plant*
(1, 8, 12, 14 – Gas-liquid separators, 2, 7, 9, 11, 13 – Heat exchangers,
3, 5, 15 – Compressors, 4 – Absorber, 6 – Pump, 10 – Desorber)

In order to assess the capital cost of the entire capture unit, the cost for each equipment involved in the process was individually calculated. For this both the physical and design characteristics were considered.

The capital cost estimates derived from this analysis take into account the installation factors for each equipment unit, ensuring the reliability and validity of the results. Equipment cost estimation was performed using numerical calculations, incorporating CAPEX indexes adjusted to reflect 2023 values. This approach ensures that the financial assessment remains accurate and relevant to current economic conditions.

Table 9 provides a detailed breakdown of the costs associated with each equipment unit.

Table 9. *Equipment units cost estimation*

Equipment	Cost estimation
Fluidised bed absorber	1.01 million €
Packed bed absorber	1.66 million €
Desorption unit	1.52 million €
Heat exchangers	0.59 million €
Pump	0.03 million €
Compressors	0.26 million €
Component separators	0.29 million €
TOTAL	3.71 million € / 4.37 million €

Table 9 shows a significant reduction in the cost of the absorption unit (40%). This translates into a cost reduction of about 15% for the entire capture unit when opting for the fluidised bed technology. This capture unit was integrated in a power plant design with a net electrical output of 1000 MW. The results of the economic analysis are presented in Table 10.

Table 10. *Techno-Economic Performance Comparison of Packed Bed (Case 1) and Fluidised Bed (Case 2) Power Plant Designs*

Key parameter	Unit	Case 1	Case 2
Net power output	MW_e	1000.00	1000.00
Net electrical efficiency	%	33.74	33.74
Carbon capture rate	%	90.00	90.00
Specific CO_2 emissions	kg/MWh	94.03	94.03
Total capital cost (CAPEX)	M€	2288.00	2169.00
Specific capital investment cost	€/kW net	2288.00	2169.00
Operational & maintenance cost (OPEX)	€/MWh	37.65	37.52
Levelized cost of electricity (LCOE)	€/MWh	97.94	95.85

The total capital cost (CAPEX) of Case 2 is lower, at 2169 M€ compared to 2288 M€ for Case 1, reflecting a reduction of approximately 5.2%. The Levelized Cost of Electricity (LCOE) is notably lower for the fluidised bed design, at 95.85 €/MWh compared to 97.94 €/MWh in the packed bed system, representing a 2.1% cost advantage.

4. Carbon capture plant control strategies

4.1 Process configuration

The carbon capture plant under consideration is designed with four interconnected subsystems: the absorber, desorber, buffer tank, and cross-heat exchanger (as shown in Figure 14). The main objective of the plant is to remove CO_2 from an incoming flue gas stream through a chemical absorption process while maintaining operational efficiency and cost-effectiveness. The system uses MEA as the solvent. The choice is based on the fact that this solvent is known for its high reactivity with CO_2 and its ability to be regenerated for repeated use.

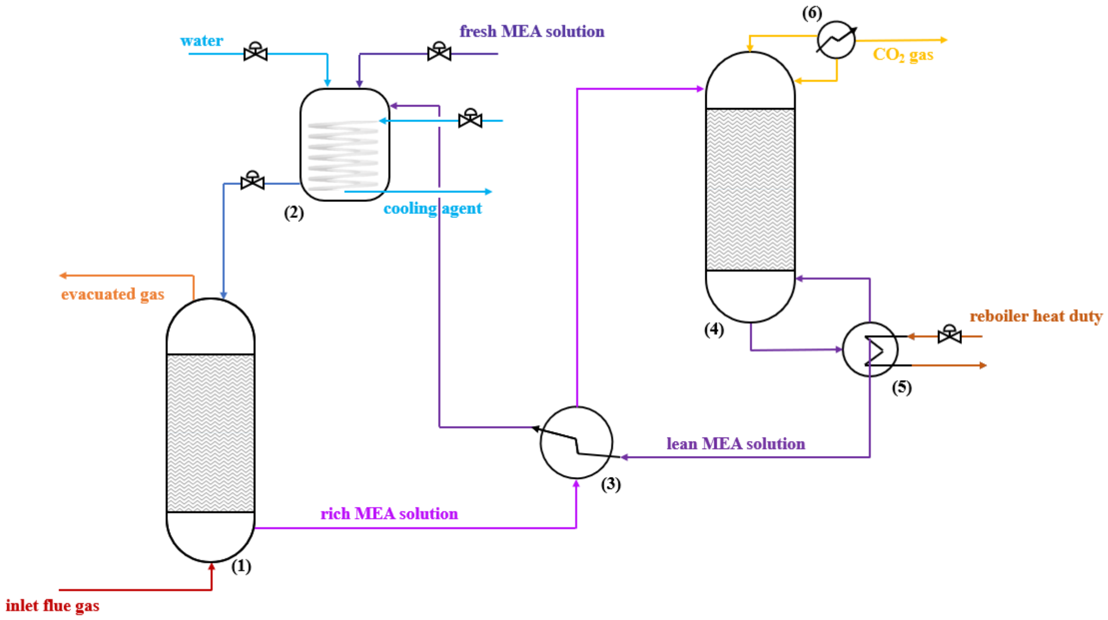

Figure 14. *Process flow diagram*

The CO_2 capture process begins in the absorber, where flue gas flows upward and contacts a downward-flowing lean MEA solution. CO_2 in the gas reacts with MEA, forming a rich solution that exits the bottom, while the treated gas leaves from the top. Before reaching the desorber, the rich MEA is preheated via a cross-heat exchanger using hot lean MEA returning from the desorber, improving energy efficiency by reducing the heating demand.

In the desorber, heat from a reboiler releases CO_2 from the MEA, which exits as gas from the top. The regenerated lean MEA collects at the bottom, is cooled, and then stored in a buffer tank before being recirculated. The buffer tank stabilizes flow and temperature, and fresh MEA and water are added as needed to maintain performance. This integrated setup enables efficient, continuous CO_2 capture with reduced energy use and operational costs.

The mathematical model developed for this study includes a comprehensive set of equations that describe the behaviour of all four interconnected subsystems: the absorber, desorber, buffer tank, and cross-heat exchanger. These equations account for mass and energy balances, thermodynamics, chemical kinetics, and transport phenomena, ensuring an accurate representation of the process at an industrial scale. By incorporating these fundamental principles, the model effectively simulates the dynamic interactions between the different units, allowing for performance optimisation. This model was then used for the incorporation of the control strategies proposed in this study.

4.1 Decentralised control strategies using PI controllers

The base of this control design is a decentralized control scheme for the buffer tank used to maintain system stability. It includes three main control loops: temperature, level and concentration control. The temperature loop regulates the tank's liquid temperature the flow of the cooling agent, ensuring optimal conditions for CO_2 absorption. The level control loop manages liquid volume to prevent overflow or depletion, adjusting the make-up water flow. The concentration control loop monitors the MEA content in the buffer tank and adjusts it to ensure that the desired concentration is maintained.

In this work, the design of the multi-loop decentralised control system prioritizes disturbance rejection as its primary objective. To address this, a cascade control structure was chosen due to its strong potential for rapid disturbance rejection. This approach enables faster response times and improved control accuracy by utilizing a secondary control loop to stabilize key process variables before disturbances propagate to the primary control loop. By implementing this strategy, the proposed control system enhances the plant's ability to maintain steady-state performance while mitigating the adverse effects of influent gas variations. The control scheme is presented in Figure 15.

The control system is structured around a cascade control strategy to ensure stable and efficient operation of the carbon capture process. At the core of this design, the master controller is responsible for maintaining the CO_2 capture (CC) rate at its desired setpoint, adjusting process conditions dynamically to counteract disturbances. The slave control loop operates in coordination with the master controller, regulating the molar flow rate ratio between lean MEA and influent CO_2. This help stabilizing the absorption process and optimizing CO_2 removal efficiency.

MEA concentration is maintained through adjustments to the fresh MEA flowrate. The buffer tank level is controlled by regulating the make-up water flowrate, ensuring stable operation. Additionally, the influent liquid temperature is managed by manipulating the cooling agent flowrate, while the reboiler liquid temperature is controlled through adjustments to the influent steam flowrate.

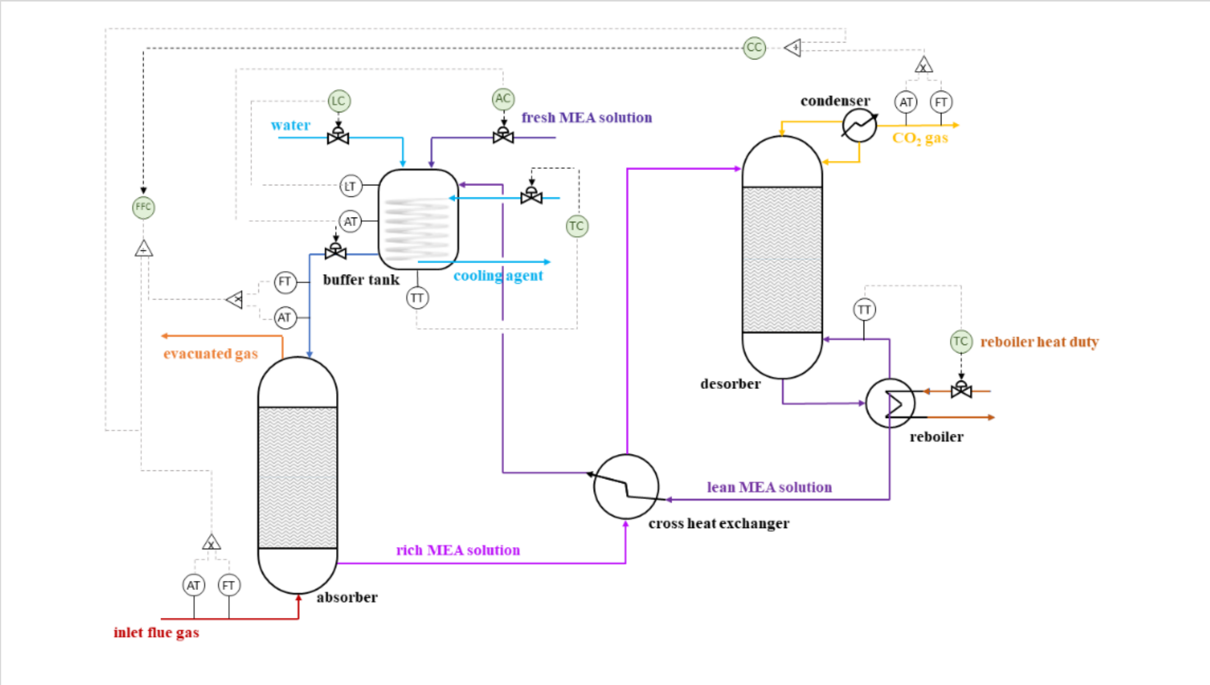

Figure 15. *Cascade decentralised control process flow diagram*

The setpoint values for the control strategies were optimized using a combination of trial-and-error and the Box-Behnken design of experiments approach. Compared to the nominal setpoints, the optimized values resulted in notable performance improvements. Specifically, the mean absolute error (MAE) of the carbon capture rate controller decreased by 43%, indicating improved precision in maintaining the target CO_2 capture efficiency. Additionally, the energy performance index was reduced by 8.3%, reflecting better energy efficiency, while a slight increase in the absorption rate further highlighted the enhanced effectiveness of the process. These results demonstrate that the optimized setpoints significantly improve both control performance and overall operational efficiency.

The control system's performance was evaluated under a dynamic disturbance scenario involving time-dependent variations in the influent flue gas flow rate. Specifically, the flow rate was programmed to first increase and then decrease, simulating typical fluctuations in electricity demand over a 24-hour cycle—conditions commonly observed in real-world power plant operations where CO_2 emissions vary with energy output. The disturbance had an amplitude of 20%, as illustrated in Figure 16, providing a realistic test of the control system’s ability to maintain stability and performance under changing operational conditions.

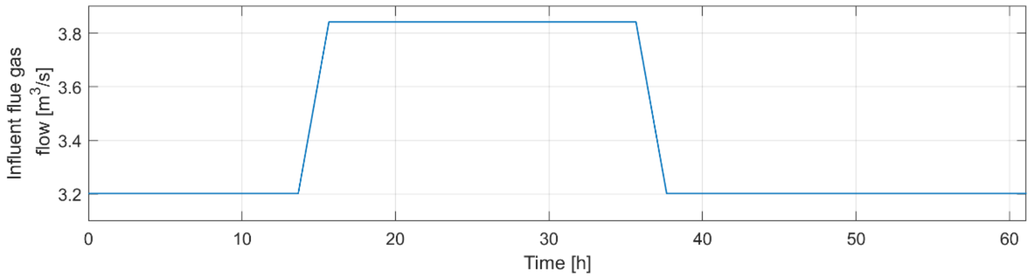

Figure 16. *Influent flue gas flowrate disturbance scenario*

The efficiency of the proposed control strategy was assessed based on its ability to restore the controlled variables to their desired setpoint values as quickly and efficiently as possible, despite the influence of the disturbance. The results are presented in the figures below.

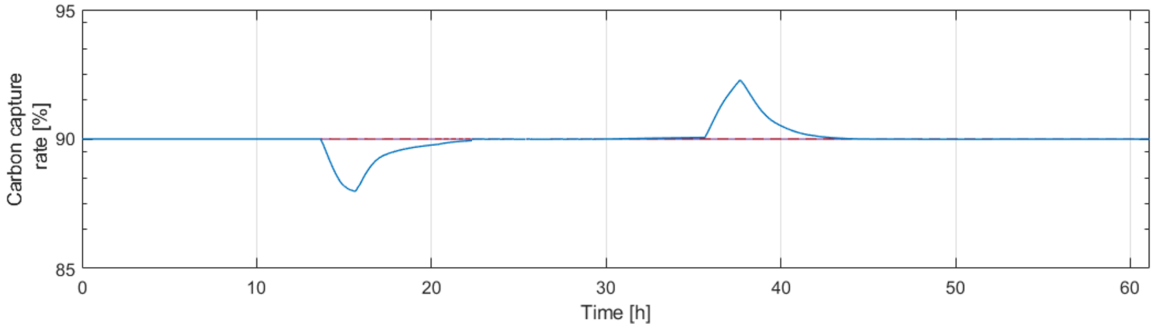

Figure 17. *Carbon capture rate controller performance (master controller)*

The cascade control system, with master and slave controllers, was assessed for setpoint tracking and disturbance rejection. It effectively kept the carbon capture rate between 85–95%, with the master controller quickly restoring the 90% setpoint by adjusting the slave controller's MEA-to-flue-gas flowrate ratio.

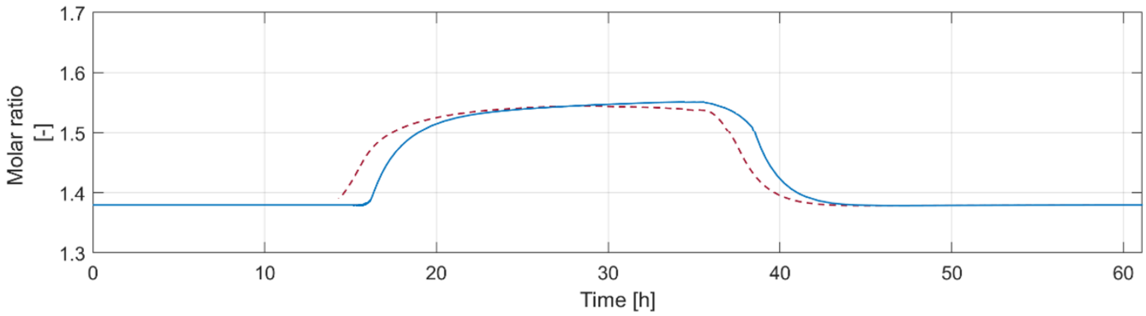

Figure 18. *Molar ratio controller performance (slave controller)*

Unlike the master controller, where the setpoint stays fixed at 90%, Figure 18 illustrates a time-varying molar ratio setpoint for the slave controller, adjusted by the master controller. A noticeable time lag appears between changes in this setpoint and the slave controller’s response, reflecting the inherent delay in cascade control systems. The plant also shows an inverse response due to the delayed feedback loop involving the absorber, desorber, heat exchanger, and buffer tank.

The performance of the buffer tank control strategy is presented in Figures 19 to 21.

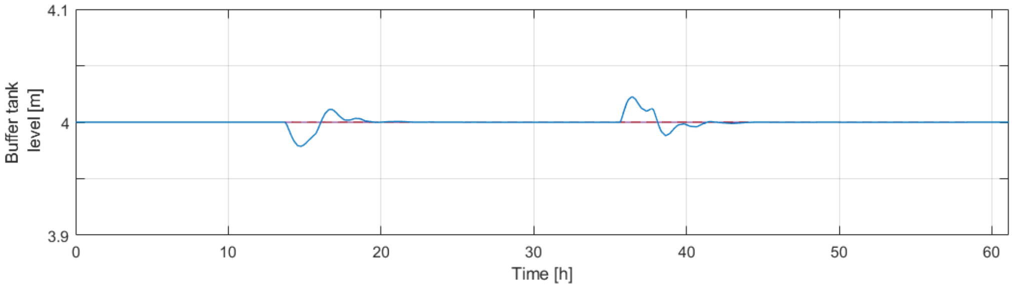

Figure 19. *Buffer tank level controller performance*

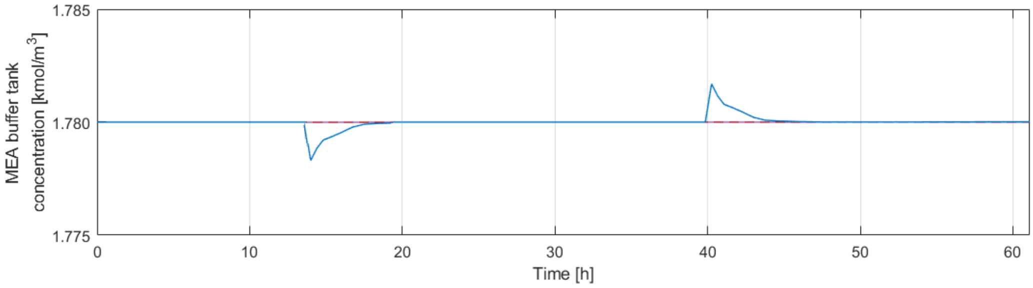

Figure 20. *Buffer tank MEA concentration controller performance*

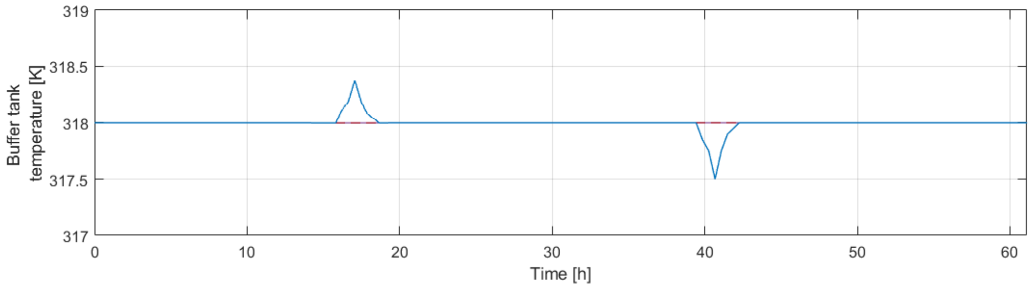

Figure 21. *Buffer tank temperature controller performance*

The control performance of the three loops used for the buffer tank is highly effective, with the buffer tank's level, MEA concentration, and temperature consistently returning to their setpoints while showing low overshoot.

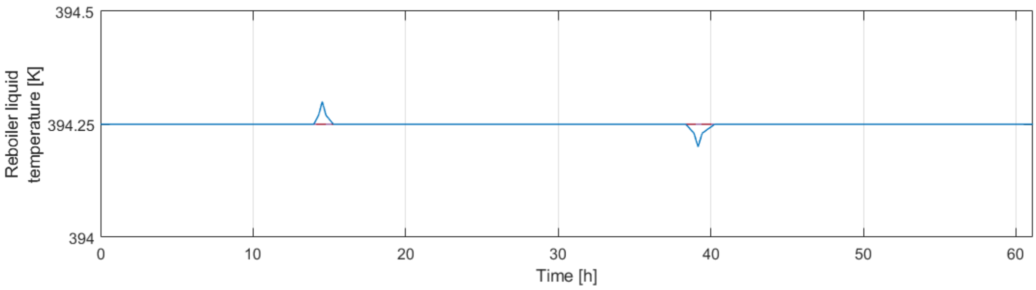

Figure 22. *Reboiler liquid temperature control loop performance*

The primary goal of the reboiler temperature control loop is to maintain the plant's energy efficiency within a desired range by adjusting the reboilers heat duty while keeping the liquid temperature at its setpoint. The very low offset and minimal overshoot that can be seen in Figure 22 show the precision of the reboiler controller. This can prove beneficial when referring to the energy efficiency of the entire system.

4.2 Hybrid PI and MPC control strategy

The proposed MPC-PI hybrid control system is specifically designed to efficiently regulate the CO_2 capture rate of the plant. Unlike many other control designs for CC plants, this approach determines the capture rate by considering the combined efficiency and dynamics of both the absorber and stripper. Table 12 provides an overview of the controlled variables, controller type, and manipulated variables. Table 4-1. Controlled and manipulated variables for hybrid control strategy

Table 2. *Controlled and manipulated variables for hybrid control strategy*

Controlled variable	Controller type	Manipulated variable
Buffer tank MEA concentration	PI	Fresh solvent flowrate
Buffer tank temperature	PI	Cooling agent flowrate
Buffer tank level	PI	Water flowrate
Carbon capture rate	MPC	Setpoint value for ratio controller
MEA to CO_2 molar flowrate ratio	PI	Inlet liquid flow to the absorber
Reboiler liquid temperature	MPC	Reboiler heat duty (steam)

The main advantage of using MPC controllers is the possibility of implementing constraints. In this case, a minimum constraint of 86% was imposed on the carbon capture rate, along with an energy performance index upper limit of 3.2.

The assessment was carried out by simulating a typical disturbance in the inlet flue gas flowrate, as shown in Figure 23. This disturbance involved a 15% increase and decrease of equal magnitude.

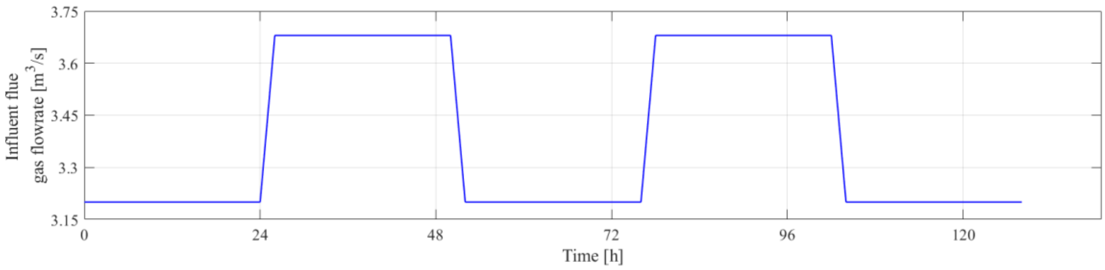

Figure 23. *Influent flue gas flowrate disturbance scenario*

The obtained results are presented below.

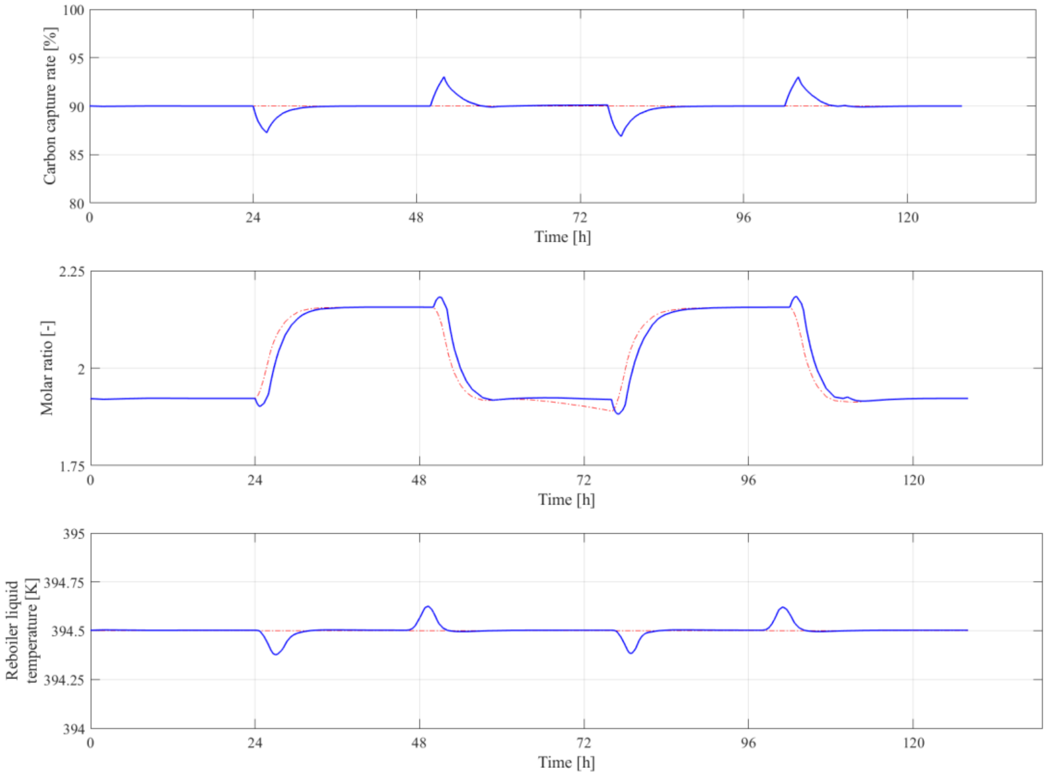

Figure 24. *MPC controller performance*

The overshoot observed in Figure 4-31 is minimal, with a deviation of less than 3.5% in both directions, and the settling time is short. Comparing this to the control results for the unconstrained case, it is evident that the CO_2 capture rate constraint applied within the MPC controller improves the overall efficiency of the carbon capture plant. These findings showcase the main advantage of using an MPC controller: the possibility of the implementation of constraints.

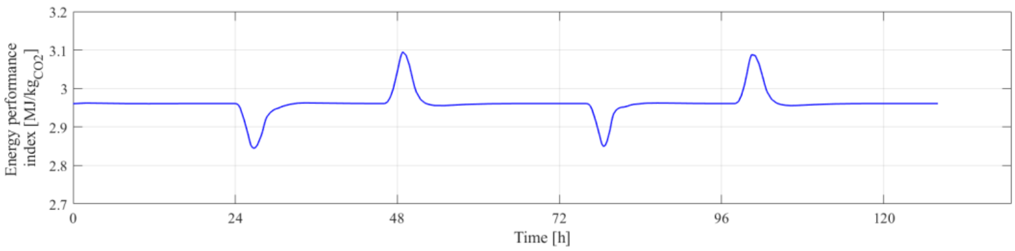

Figure 25. *Energy performance index*

As shown in Figure 4-33, the energy performance index remains below 3.1 MJ/kg$_{CO2}$ at all times, even in the presence of the disturbance. This highlights the effectiveness of the MPC controller and its ability to successfully meet operational constraints,

5. Concluding remarks

This thesis was focused on the presentation and analysis of two directions that can be followed in order to improve the overall performance of carbon capture plants: process intensification and control system implementation. The first one involves a new carbon capture technology that uses three-phase fluidisation in the absorption column. The second one involves the addition of control loops to existing capture plants in order to maximise capture efficiency and minimise energy consumption.

The purpose of this thesis, as stated in Section 1.2, is: i) to analyse, assess and compare the performance of existing carbon capture technologies with a novel approach, involving three-phase fluidisation by using mathematical models and ii) to develop and simulate the implementation of control strategies for carbon capture processes.

Chapter 1 of this thesis presents a comprehensive review on literature references regarding not only existing carbon capture technologies (i.e. working principles, solvents used, contacting methods), but also control strategies available and their respective applicability in carbon capture processes.

The first goal of this thesis was the object of Chapter 3. The experimental analysis on the proposed process, presented in this section shows the way gas-solid-liquid systems behave in two different scenarios: water-air system and NaOH aqueous solution – air/CO_2 mixture. The first one is used to highlight the hydrodynamics of such a process, while the second one is used to underscore the intensified mass transfer between the gas and the liquid phases. The analysis results lead to two important conclusions: i) this type of absorber presents lower values of pressure drop than regular packed bed columns, hence less flow resistance in the system and ii) the effective mass transfer area is 5-6 times greater in this case than in regular packed bed columns.

The developed mathematical model for the gas-solid-liquid fluidised bed absorber focuses on all phenomena that take place within the absorption column (i.e. mass transfer, hydrodynamic, reaction kinetics, mass and energy conservation principles). The model was validated against experimental data with good correlation results ($R>0.9$) for all considered parameters: fluidised bed expansion, pressure drop, effective mass transfer area, carbon capture efficiency.

A comparison of the proposed system with the traditional packed bed columns was performed. The results show a significant difference between fluidised bed columns and packed bed columns in terms of effective mass transfer area (i.e. 5-8 times higher values of the effective mass transfer area in fluidised bed absorbers) and also 8-10 times higher values for the partial mass transfer coefficients and implicitly the CO_2 transferred flow between the gas and the liquid phases. Moreover, these findings highlight the fact that in case of using fluidised bed absorbers, the gas velocity needs to be only slightly higher than the minimum fluidisation velocity for the required level of turbulence to be achieved. This, in return, could translate into a higher gas treating capacity.

For the scale-up analysis a comprehensive investigation was conducted on different plant configurations. These configurations were chosen in order to determine the optimal static bed height, the particle density and particle diameter and their distribution on column trays. The studies show that a three-tray configuration works best, with descending static bed height. Also, decreasing solid particles size could be beneficial, as long as the bed-lift phenomenon is avoided.

The economic analysis was completed in Section 3.7 of this thesis. The results show that the use of a fluidised bed column leads to a 40% decrease of the absorber capital cost, 15% cost reduction of the capture unit and 2.1% reduction in the cost for electricity production.

The second goal of this thesis was the object of Chapter 4. This chapter presents a detailed analysis of several control strategies: i) PI decentralised control, ii) Cascade control strategy and iii) Hybrid PI-MPC control strategy. The results show the advantages of using some form of control design to ensure flexible and smooth operation despite disturbances.

The study introduced a comprehensive hybrid control strategy aimed at effectively managing key variables of the carbon capture processes, particularly the CO_2 capture yield and the temperature of the liquid phase in the reboiler, alongside regulating the buffer tank variables, all devoted to sustaining the efficient and smooth operation of the absorber-desorber units. This control approach integrated the multivariable model predictive control with the operation of the buffer tank decentralized control loops.

The setpoint optimisation was conducted by the Design of Experiment method, using Box-Behnken Design. The new-found setpoint values improved the plant's performance, reducing the mean absolute error of the carbon capture rate by 24%, enhancing the energy performance index by 3%, and maintaining the absorption rate above 92%.

This study demonstrated the effectiveness of the fluidized bed absorption system and proposed directions for improving its performance and stability through mechanical and operational enhancements. Mechanically, incorporating agitators at each stage of the absorption unit can ensure uniform fluidization and prevent issues like flow maldistribution and the piston effect, especially in multi-stage, three-phase systems where low-density solids are used. These agitators require minimal energy and have little impact on hydrodynamics, offering a practical solution to enhance mass transfer. Operationally, the development of control strategies focused on key process variables, such as bed height and pressure drop, can help maintain steady-state performance under dynamic conditions by adjusting flue gas flow and velocity. These measures aim to prevent defluidization, ensure consistent absorber operation, and support reliable, efficient system control, forming a solid foundation for future research and optimization.

References

1. Jeffry L, Ong MY, Nomanbhay S, Mofijur M, Mubashir M, Show PL. Greenhouse gases utilization: A review. *Fuel* 2021;301:121017. https://doi.org/10.1016/j.fuel.2021.121017.
2. Dumitran GE, Vuta LI, Negrusa E, Birdici AC. Reducing greenhouse gas emissions in Romanian agriculture using renewable energy sources. *J Clean Prod* 2024;467:142918. https://doi.org/10.1016/j.jclepro.2024.142918.
3. Duro JA. Intercountry inequality on greenhouse gas emissions and world levels: An integrated analysis through general distributive sustainability indexes. *Ecol Indic* 2016;66:173–179. https://doi.org/10.1016/j.ecolind.2016.01.026.
4. Erdogan S, Pata UK, Solarin SA, Okumus I. On the persistence of shocks to global CO_2 emissions: A historical data perspective (0 to 2014). *Environ Sci Pollut Res* 2022;29(51):77311–77320. https://doi.org/10.1007/s11356-022-21278-8.
5. Bala A, Raugei M, Benveniste G, Gazulla C, Fullana-i-Palmer P. Simplified tools for global warming potential evaluation: when 'good enough' is best. *Int J Life Cycle Assess* 2010;15:489–498. https://doi.org/10.1007/s11367-010-0153-x.
6. Intergovernmental Panel on Climate Change. 2006 IPCC guidelines for national greenhouse gas inventories. IGES; 2006. https://www.ipcc-nggip.iges.or.jp/public/2006gl/.
7. Reiter G, Lindorfer J. Evaluating CO_2 sources for power-to-gas applications–A case study for Austria. *J CO_2 Util* 2015;10:40–49. https://doi.org/10.1016/j.jcou.2015.03.003.
8. Friedlingstein P, O'Sullivan M, Jones MW, Andrew RM, Bakker DCE, Hauck J, et al. Global carbon budget 2024. *Earth Syst Sci Data* 2025;17(2):965–1042. https://doi.org/10.5194/essd-17-965-2025.
9. Intergovernmental Panel on Climate Change. Sixth Assessment Report (AR6); 2021. https://www.ipcc.ch/report/sixth-assessment-report-cycle/ (accessed January 25, 2025).
10. Carbon Brief. Analysis: Global CO_2 emissions will reach new high in 2024 despite slower growth. *Carbon Brief*; 2024. https://www.carbonbrief.org/analysis-global-co2-emissions-will-reach-new-high-in-2024-despite-slower-growth/ (accessed January 25, 2025).
11. Liu Z, Ciais P, Deng Z, Lei R, Davis SJ, Feng S, et al. Near-real-time monitoring of global CO_2 emissions reveals the effects of the COVID-19 pandemic. *Nat Commun* 2020;11:5172. https://doi.org/10.1038/s41467-020-18922-7.

12. Wu Q, Chen Y, Huang C, Zhang L, He C. Carbon emission peaks in countries worldwide and their national drivers. *Carbon Res* 2025;4(1):28. https://doi.org/10.1007/s44246-025-00195-8.
13. Astanakulov O, Asatullaev K, Saidaxmedova N, Batirova N. The energy efficiency of the national economy assessment in terms of investment in green energy. *Econ Ann XXI* 2021;189. https://doi.org/10.21003/ea.V189-03.
14. Baptista LB, Schaeffer R, van Soest HL, Fragkos P, Rochedo PR, van Vuuren D, et al. Good practice policies to bridge the emissions gap in key countries. *Glob Environ Change* 2022;73:102472. https://doi.org/10.1016/j.gloenvcha.2022.102472.
15. United Nations Environment Programme. Emissions Gap Report 2024: No more hot air... please! UNEP; 2024. https://www.unep.org/resources/emissions-gap-report-2024. (accessed January 25, 2025)
16. Stechemesser A, Koch N, Mark E, Dilger E, Klösel P, Menicacci L, et al. Climate policies that achieved major emission reductions: Global evidence from two decades. *Science* 2024;385(6711):884–892. https://doi.org/10.1126/science.adl6547.
17. Dey S, Sreenivasulu A, Veerendra GTN, Rao KV, Babu PA. Renewable energy present status and future potentials in India: An overview. *Innov Green Dev* 2022;1(1):100006. https://doi.org/10.1016/j.igd.2022.100006.
18. Hassan Q, Viktor P, Al-Musawi TJ, Ali BM, Algburi S, Alzoubi HM, et al. The renewable energy role in the global energy transformations. *Renew Energy Focus* 2024;48:100545. https://doi.org/10.1016/j.ref.2024.100545.
19. Yolcan OO. World energy outlook and state of renewable energy: 10-Year evaluation. *Innov Green Dev* 2023;2(4):100070. https://doi.org/10.1016/j.igd.2023.100070.
20. Maradin D. Advantages and disadvantages of renewable energy sources utilization. *Int J Energy Econ Policy* 2021;11(3):176–183.
21. Chen S, Liu J, Zhang Q, Teng F, McLellan BC. A critical review on deployment planning and risk analysis of carbon capture, utilization, and storage (CCUS) toward carbon neutrality. *Renew Sustain Energy Rev* 2022;167:112537. https://doi.org/10.1016/j.rser.2022.112537.
22. Popielak P, Majchrzak-Kucęba I, Wawrzyńczak D. Climate change mitigation with CCUS—A case study with benchmarking for selected countries in adapting the European Union's Green Deal. *Int J Greenh Gas Control* 2024;132:104057. https://doi.org/10.1016/j.ijggc.2023.104057.

23. Dávila JG, Sacchi R, Pizzol M. Preconditions for achieving carbon neutrality in cement production through CCUS. *J Clean Prod* 2023;425:138935. https://doi.org/10.1016/j.jclepro.2023.138935.
24. Dubey A, Arora A. Advancements in carbon capture technologies: A review. *J Clean Prod* 2022;373:133932. https://doi.org/10.1016/j.jclepro.2022.133932.
25. Li J, Zhang H, Gao Z, Fu J, Ao W, Dai J. CO_2 capture with chemical looping combustion of gaseous fuels: an overview. *Energy Fuels* 2017;31(4):3475–3524. https://doi.org/10.1021/acs.energyfuels.6b03204.
26. Chisalita DA, Cormos CC. Techno-economic assessment of hydrogen production processes based on various natural gas chemical looping systems with carbon capture. *Energy* 2019;181:331–344. https://doi.org/10.1016/j.energy.2019.05.179.
27. Sabatino F, Grimm A, Gallucci F, van Sint Annaland M, Kramer GJ, Gazzani M. A comparative energy and costs assessment and optimization for direct air capture technologies. *Joule* 2021;5(8):2047–2076. https://doi.org/10.1016/j.joule.2021.05.023.
28. McQueen N, Gomes KV, McCormick C, Blumanthal K, Pisciotta M, Wilcox J. A review of direct air capture (DAC): scaling up commercial technologies and innovating for the future. *Prog Energy* 2021;3(3):032001. https://doi.org/10.1088/2516-1083/abf1ce.
29. Li K, Leigh W, Feron P, Yu H, Tade M. Systematic study of aqueous monoethanolamine (MEA)-based CO_2 capture process: Techno-economic assessment of the MEA process and its improvements. *Appl Energy* 2016;165:648–659. https://doi.org/10.1016/j.apenergy.2015.12.109.
30. Hamdy LB, Goel C, Rudd JA, Barron AR, Andreoli E. The application of amine-based materials for carbon capture and utilisation: an overarching view. *Mater Adv* 2021;2(18):5843–5880. https://doi.org/10.1039/d1ma00360g.
31. Zhao S, Feron PH, Cao C, Wardhaugh L, Yan S, Gray S. Membrane evaporation of amine solution for energy saving in post-combustion carbon capture: wetting and condensation. *Sep Purif Technol* 2015;146:60–67. https://doi.org/10.1016/j.seppur.2015.03.015.
32. Keil FJ. Process intensification. *Rev Chem Eng* 2018;34(2):135–200. https://doi.org/10.1515/revce-2017-0085.
33. Dragan S. Calculation of the effective mass transfer area in turbulent contact absorber. *Studia UBB Chemia* 2016;61(3, Tom I):227–238.

34. Pahija E, Golshan S, Blais B, Boffito DC. Perspectives on the process intensification of CO_2 capture and utilization. *Chem Eng Process Process Intensif* 2022;176:108958. https://doi.org/10.1016/j.cep.2022.108958.

35. Ullah A, Amanat A, Imran M, Gillani SSJ, Kilic M, Khan A. Effect of turbulence modeling on hydrodynamics of a turbulent contact absorber. *Chem Eng Process Process Intensif* 2020;156:108101. https://doi.org/10.1016/j.cep.2020.108101.

36. Wu X, Wang M, Liao P, Shen J, Li Y. Solvent-based post-combustion CO_2 capture for power plants: A critical review and perspective on dynamic modelling, system identification, process control and flexible operation. *Appl Energy* 2020;257:113941. https://doi.org/10.1016/j.apenergy.2019.113941.

37. MathWorks. MATLAB Documentation. 2021.

38. Chemstations. CHEMCAD Physical properties: User's Guide. 2004.

39. Montgomery DC, Peck EA, Vining GG. *Introduction to Linear Regression Analysis.* John Wiley & Sons; 2021.

40. Jankovic A, Chaudhary G, Goia F. Designing the design of experiments (DOE)–An investigation on the influence of different factorial designs on the characterization of complex systems. *Energy and Buildings* 2021;250:111298. https://doi.org/10.1016/j.enbuild.2021.111298.

41. Thokchom B, Radhapyari K, Dutta S. Occurrence of trihalomethanes in drinking water of Indian states: A critical review. In: Prasad MNV, editor. *Disinfection By-products in Drinking Water* (pp. 83–107). Butterworth-Heinemann; 2020. http://dx.doi.org/10.1016/B978-0-08-102977-0.00004-4.

42. Cormos, C.-C., Dinca, C., Techno-economic and environmental implications of decarbonization process applied for Romanian fossil-based power generation sector, Energy, 220, 119734, 2021. https://doi.org/10.1016/j.energy.2020.119734.

43. Hassini, E., Surti, C., & Ehsani, M. (2012). A review of environmental performance indices. International Journal of Environmental Science and Technology, 9(3), 493-506.

44. Dragan S. Calculation of the effective mass transfer area in turbulent contact absorber. Studia UBB Chemia 2016;61(3):227–238.

45. Billet, R., Schultes, M., "Predicting mass transfer in packed columns," *Chem. Eng. Technol.*, 16(1), 1–9, 1993. https://doi.org/10.1002/ceat.270160102

46. Rocha JA, Bravo JL, Fair JR. Distillation columns containing structured packings: A comprehensive model for their performance. 1. Hydraulic models. *Ind Eng Chem Res* 1993;32(4):641–651. https://doi.org/10.1021/ie00016a010.